AUT Journal of Civil Engineering

AUT J. Civil Eng., 4(2) (2020) 229-240
DOI: 10.22060/ajce.2019.16184.5574

Numerical Modeling of Hydraulic Properties of Sloped Broad Crested Weir

Rasoul Daneshfaraz [1,*], Mehdi Dasineh[2], Amir Ghaderi[3], Sina Sadeghfam[4]

[1] Professor, Department of Civil Engineering, Faculty of Engineering, University of Maragheh, Maragheh, East Azerbaijan, Iran.
[2] M.Sc. Graduate, Department of Civil Engineering, Faculty of Engineering, University of Maragheh, Maragheh, East Azerbaijan, Iran.
[3] Ph.D. Student, Department of Civil Engineering, Faculty of Engineering, University of Zanjan, Zanjan, Iran.
[4] Assistant Professor, Department of Civil Engineering, Faculty of Engineering, University of Maragheh, Maragheh, East Azerbaijan, Iran.

ABSTRACT: In this study, Numerical modeling of hydraulic properties of sloped broad crested weir is numerically investigated. In order to simulate the free surface flow, the Volume of Flow (VOF) method was used. Turbulence models employed in these simulations were RNG k-ε, and standard k-ε models. The results indicate that RNG k-ε model is more accurate in simulating the flow surface profile of the broad crested weir than the standard k-ε turbulence model. By sloping the crest, the flow depth decreases at the downstream of the weir. At the adverse slope, flow velocity toward the downstream of the crest decrease and flow depth increases. In addition, it was observed that in horizontal or positive slope crests, the control section take place over the crest while for the adverse slope, the control section is slightly shifted toward the upstream of the crest. This could be due to the separation of the flow at the apex of the crest. Moreover, the average Froude number increases for a constant slope (adverse or positive) in the downstream of the weir. It was concluded that the total energy at the downstream of the weir is not a function of the crest slope. The energy increases with the height of the weir and flow discharge. The highest amount of the total energy in downstream of the weir occurs for discharges of 3, 4.7 and 6 lit/s with the slopes of 4:1, 4:-1, 8:-1 and are 0.244, 0.317 and 0.452, respectively.

Review History:
Received: 2019-04-22
Revised: 2019-05-14
Accepted: 2019-05-16
Available Online: 2019-05-16

Keywords:
Broad crested weir
Crest slope
Control section
Total energy

1. INTRODUCTION

Weirs, commonly made of concrete, are used to control, adjust, and measure the flow rate. Broad-crested weirs are common weirs, preferred in irrigation systems due to their low sensitivity to submergence, simple geometry and low construction costs. The geometry of broad-crest weirs can influence the flow conditions and discharge capacity. Numerous experimental and numerical researches have been conducted on the flow over broad-crest weirs including, and notr limited to, Doeringsfeld and Baker [1], Tracy [2], Henderson [3], Rao and Shukla [4], Bos et al. [5], Ramamurty et al. [6], Hager and Schwalt [7], Fritz and Hager [8], Johnson [9]. Farhoudi and Shahalami [10] demonstrated the results of experimental work carried out on rectangular broad crested weir with sloped upstream face to investigate the effect of the upstream slope on discharge efficiency. It is revealed that the slope of the upstream face in rectangular broad crested weir would smoothen the flow profile having the critical depth on the weir crest adjacent and upstream or downstream edge of the weir. Gogus et al. [11] investigate the effects of the width of the lower weir crest and step height of broad-crested weirs of the rectangular compound cross section on the values of the discharge coefficient. For this purpose, nine different broad-crested weir models with rectangular compound cross-sections and a model with a rectangular cross-section was tested in a horizontal laboratory flume with wide range of discharges. The relation between the discharge coefficient and other parameters was investigated, and these quantities were compared with those of the broad-crested weir models with a rectangular cross section. Hargreaves et al. [12] simulated the water surface profile in a broad-crest weir using VOF technique. Farhoudi and Shokri [13] experimentally determined the characteristic of flow over the rectangular sloped broad-crest weir. They have considered the downward slope effects on weir discharge efficiency and its sensitivity to downstream submersion ratios. Sargison and Percy [14] investigated the flow of water over a trapezoidal, broad-crested, or embankment weir with varying upstream and downstream slopes has been investigated. Data are presented comparing the effect of slopes of 2H: 1V, 1H: 1V and vertical in various combinations on the upstream and downstream faces of the weir. The results showed that increasing the upstream slope to the vertical decreased the height of the surface profile and, hence, the static pressure of the crest. Varying the downstream slope had a negligible effect on the surface and pressure profiles over the weir. Goodarzi et al. [15] studied the characteristic of flow over a broad-crest weir with different upstream slopes. The results showed that decreasing the upstream slope, increases the discharge coefficient and dissipate the separation zone. Hoseini [16] carried out an experimental study on the flow over the

*Corresponding author's email: daneshfaraz@yahoo.com

triangular broad-crest weir. The results indicated Froude number and h_1/L (h_1 is the total energy in the upstream of the weir, L is the length of the weir) are effective parameters in the estimation of flow discharge coefficient. Torabi et al. [17] experimentally investigated the trapizoidal foundation profile. Tănase et al. [18] experimentally and numerically studied the free surface flow on a broad-crest weir for a smooth and patterned surface. They used Fluent software and RNG k-ε turbulence model for numerical study. The results showed that the patterned surface influences the flow separation area. They also proved that the vortex area in the downstream of the weir with the patterned crest is smaller than a smooth surface. Mohammadzadeh-Habili et al. [19] experimentally investigated finite crest length weir and quarter-circular crested weir and hydraulic characteristics of two weirs were compared together. Depending on the ratio of total upstream head H to weir crest length L, flow over the finite crest length weir was undular, parallel to the crest surface or curvilinear. Result indicates that quarter-circular crested weir is less sensitive to cavitation danger. Xu and Jin [20] studied the flow over the broad–crest weir using the meshless (MPS) method for different discharges coefficient and upstream slopes. At the end, the results were compared with experimental methods, and a good agreement was reported. Parsaie et al. [21] studied the group method of data handling (GMDH) trained by particle swarm optimization technique was used to predict the discharge coefficient of cylindrical weir-gate. The performances of the prepared GMDH model were compared with the multi-layer perceptron neural network (MLPNN) and support vector machine (SVM) that developed to this end, as well. Results indicated that all developed models have suitable performance, however; the SVM model was a bit more accurate. Daneshfaraz et al. [22] studied the flow over a broad-crest weir with or without an opening in the body of the weir with different slopes using Flow-3D software. The results showed that the opening in the body of the weir leads into an increase in discharge coefficient and a decrease in water level in the upstream.

Reviewing the literature shows that up to now the effect of slope of the crest on hydraulic properties has not been investigated. In this study, Numerical modeling of hydraulic properties of sloped broad crested weir was numerically investigated. Changes in the slope of the weir's crest affect the location of the critical depth. Since in practice, knowing the specific location of the critical depth leads to an accurate estimation of the flow rate, the main purposes of this study were to find the critical depth location on the broad-crested weir as well as the effect of the sloped crest on this location. In addition, the behavior of the water surface profile and the total energy are described in this paper.

2. METHODS AND MATERIALS

2-1- Effective parameters

The hydraulic and geometric parameters affecting the broad-crest weirs by sloping the crest are the relation (1):

$$\varphi = f_1(H_0, h_0, y_0, Q, y_c, L_w, S, \theta, g, \rho, \mu) \quad (1)$$

Using the Buckingham theorem and choosing S, Q, μ repeat parameters, the relation (2) is obtained:

$$\varphi = f_2\left(\frac{H_0}{S}, \frac{h_0}{S}, \frac{y_0}{S}, \frac{y_c}{S}, \frac{L_w}{S}, \theta, \frac{gS^5}{Q^2}, \frac{\rho Q}{\mu S}\right) \quad (2)$$

Considering that the dimensionless expressions $\frac{\rho Q}{\mu S}$ and $\frac{gS^5}{Q^2}$ are equivalent to the Reynolds and Froude numbers, respectively, and on the other hand, with respect to the turbulence of the flow across the simulation, and to ignore the Reynolds number according to (3) will have:

$$\varphi = f_3\left(\frac{H_0}{S}, \frac{h_0}{S}, \frac{y_0}{S}, \frac{y_c}{S}, \frac{L_w}{S}, \theta, \frac{1}{Fr^2}\right) \quad (3)$$

Where, H_0 energy head, h_0 water depth at upstream of the weir, y_0 is the approach weir depth, Q weir flow discharge, y_c critical depth on the weir crest, L_w length of weir crest, S the height of weir, θ the ratio of the vertical slope to the horizontal slope, g Earth's gravity acceleration, ρ density, μ Dynamic viscosity.

Fig. 1 shows the schematic view of broad-crest weir with a sloped crest with effective parameters.

2-2- Governing equations

The dynamic behavior can be described by a set of equations known as the St. Venant equations [23]. Also equations governing a viscous incompressible fluid in a turbulent state are expressed by in depth averaged Navier-Stokes equations, so called Reynolds, which include the equations of continuity and motion [24].

$$\frac{\partial \rho}{\partial t} + \frac{\partial (\rho u_i)}{\partial x_i} = 0 \quad (4)$$

$$\frac{\partial u_i}{\partial t} + u_j \frac{\partial u_i}{\partial x_i} = -\frac{1}{\rho}\frac{\partial P}{\partial x_i} + g_i + \frac{\partial}{\partial x_j} S_j \quad (5)$$

In the above equations u_i is the rate factor in the direction x_i, P is the total pressure, ρ is the fluid density, g_i is the velocity gravity in xi direction, S_{ij} is the stress tensor. These can be expressed as the following equation for the turbulent flow [24].

$$S_{ij} = \left[\rho(v + v_t)\left(\frac{\partial u_i}{\partial x_j} + \frac{\partial u_j}{\partial x_i}\right)\right] - \left[\frac{2}{3}\rho(k + v_t)\frac{\partial u_i}{\partial x_i}\delta_j\right] \quad (6)$$

In the above equations, v_t is the eddy viscosity which is a function of flow and turbulence characteristics. S_{ij} is used for application of eddy viscosity definition. Turbulent kinetic energy per mass unit is expressed by equation 8.

$$\delta_{ij} = \begin{cases} 1 & i = j \\ 0 & i \neq j \end{cases} \quad (7)$$

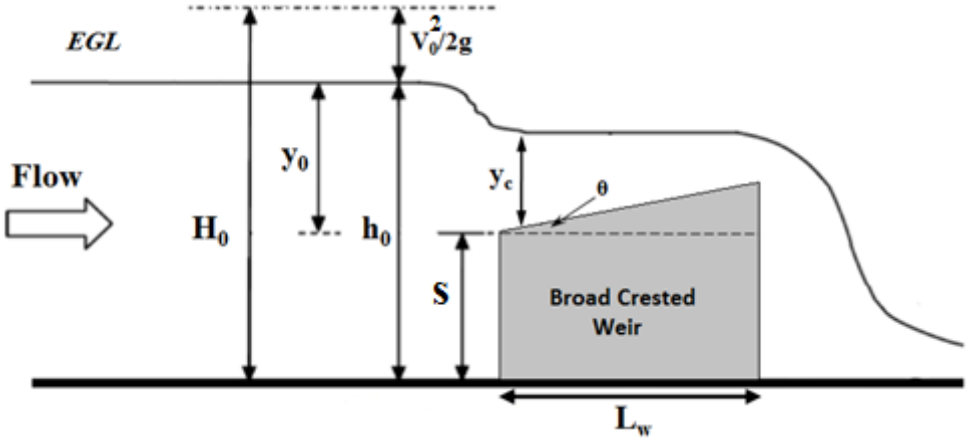

Fig. 1. Broad-crest weir with a sloped crest

Table 1. The Coefficients for standard k-ε and RNG k-ε turbulence models

Turbulence Models	$C_{4\varepsilon}$	$C_{1\varepsilon}$	$C_{2\varepsilon}$	σ_k	σ_ε
k-ε	0.09	1.44	1.92	1.00	1.30
RNG k-ε	0.08	1.42	1.68	0.72	0.72

$$k = \frac{1}{2}\left(\overline{u_i'}^2 + \overline{u_j'}^2 + \overline{u_k'}^2\right) \quad (8)$$

In this study, standard k-ε and RNG k-ε turbulence models are used. These models propose transformation equations for turbulent kinetic energy (k) and dissipation of kinetic energy of turbulence (ε). The main difference between these two turbulent models is the equations to determine ε. In higher Reynolds numbers, where the flow is fully turbulent and the effect of the molecular viscosity is negligible, the standard k-ε model is preferable. In the RNG k-ε model, an extra term in equation ε increases the computational accuracy of the model where the fluid flow with large strains occurs (e.g. flow in arc boundary layers and diverging flow).

$$\frac{\partial(\rho k)}{\partial t} + \frac{\partial(\rho k u_i)}{\partial x_i} = \frac{\partial}{\partial x_j}\left[(\mu + \frac{\mu_t}{\sigma_k})\frac{\partial k}{\partial x_j}\right] + 2\mu_t E_{ij} E - \rho\varepsilon \quad (9)$$

$$\frac{\partial(\rho\varepsilon)}{\partial t} + \frac{\partial(\rho\varepsilon u_i)}{\partial x_i} = \frac{\partial}{\partial x_j}\left[(\mu + \frac{\mu_t}{\sigma_\varepsilon})\frac{\partial \varepsilon}{\partial x_j}\right] +$$

$$C_{1\varepsilon}\frac{\varepsilon}{k} 2\mu_t E_{ij} E_{ij} - C_{2\varepsilon}^{*}\rho\frac{\varepsilon^2}{k} \quad (10)$$

In these equations,

$$C_{2\varepsilon}^{*} = C_{2\varepsilon} + \frac{C_\mu \eta^3 (1 - \eta/\eta_0)}{1 + \beta\eta^3} \quad (11)$$

$$\eta = \frac{Sk}{\varepsilon} \quad (12)$$

$$S = \sqrt{2S_{ij}S_{ij}} \quad (13)$$

$$S_{ij} = \frac{1}{2}\left(\frac{\partial u_i}{\partial x_j} + \frac{\partial u_j}{\partial x_i}\right) \quad (14)$$

The values used for these coefficients in the present study are given in Table 1[25].

In this study, the volume of fluid (VOF) method was used to simulate free surface. VOF techniques usually used to model 2-phase flows. In each fluid cell, a variable function called α indicates the fraction of each fluid in the computational cell is used. For instance, in water-air interaction, α equal to 1 indicates the cell full of water while zero means the cell is full of air. For 0< α 1<shows the fraction of the cell filled with water [26]. Therefore, the free surface over the water flow can be determined by cells with α<1. In this study, $\alpha \leq 0.5$ was the criterion to define the free surface of the water body. The value of α in each cell was computed through Eq. [15].

$$\frac{\partial\alpha}{\partial t} + u\frac{\partial\alpha}{\partial x} + v\frac{\partial\alpha}{\partial y} = 0 \quad (15)$$

2-3- Characteristic of the numerical model and the solution field

In this research, Fluent software employed to investigate on the effects of sloped-crest weir on the hydraulic characteristics of the flow such as discharge coefficient, Froude number, the location of the critical depth (flow control section) and total energy.

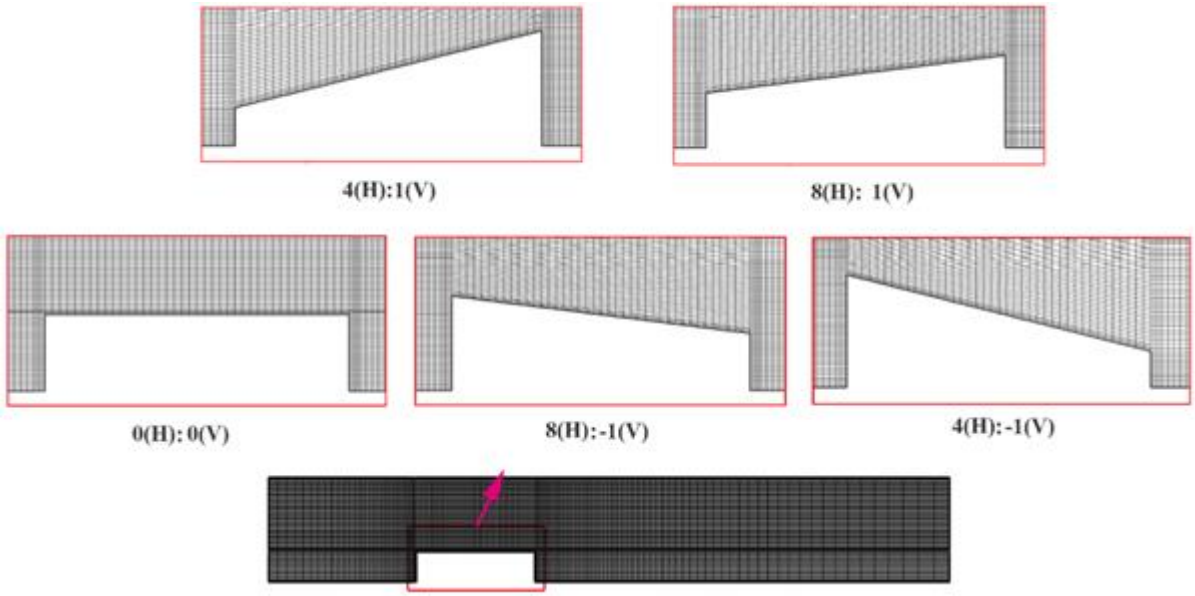

Fig. 2. The investigated broad-crest weir with different slopes of the crest and gridding

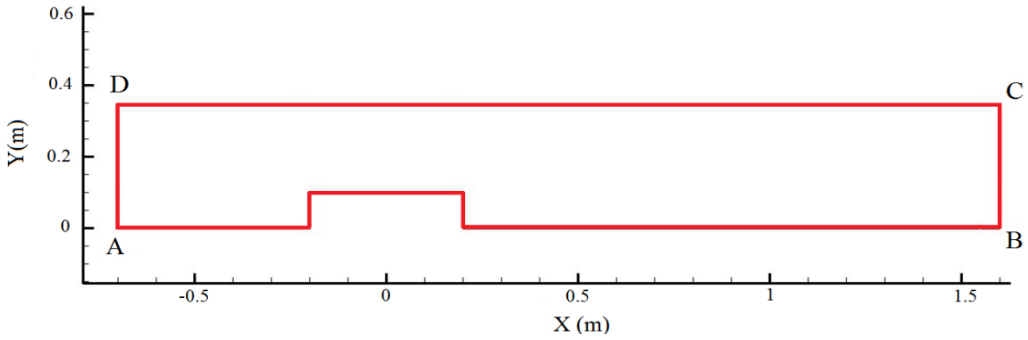

Fig. 3. The cross section of the model

Experimental data of the rectangular broad-crest weir (Sarker and Rhodes [27]) was used to validate the findings. Four different slopes were applied to weir crest including 4:1, 8:1, 4:-1, 8:-1, and 0:1 (H:V)(Fig. 2). Table 2 shows the governing conditions of the present study. The computational domain is non-uniform in depth and finer mesh was used near the walls. The distance of the first cell from the wall was selected in a way the first cell located within the viscous Layer. In this regards, the dimensionless y^+ was defined as the following equation remained less than 5.

$$y^+ = \frac{y_1\sqrt{\tau/\rho}}{\nu} \tag{16}$$

Where, y_1 is the perpendicular distance from the center of the cell to the wall, τ is the shear stress over the wall, and ν is the kinematic viscosity. Structured quadrilateral grids were generated for the computational domain using Gambit software. For the sake of the speed and accuracy of the simulation. Fig. 2 illustrates the mesh throughout the computational domain.

One of the most important steps in numerical simulation is to defin the boundary conditions. The boundary conditions were appliedto the model in accordance with the experiments using Gambit software (Fig. 3).

According to Fig. 3, the Y-min (AB) boundary condition, which consists of the channel bed, and the broad-crested weir's body, considered as wall where non-slip condition is considered in Fluent software default for this type of boundary. The inlet boundary condition (AD) considered as Pressure- Inlet with constant flow depth according to the fact that the inflow depth of the upstream are known and constant. *X*-max (BC) boundary considered as pressure outlet and the *Y*-max (CD) considered as symmetry with zero fraction of fluid. Table 3 shows the boundary conditions for the broad-crested sloped weir.

3. RESULTS AND DISCUSSION

3-1- Turbulence model selection and numerical model verification

In this study, water level surface profiles of numerical study has been verified with Sarker and Rhodes [26] experimental data. Fig. 4 and 5 shows the water-air contours of volume fraction and the water surface profile over the rectangular

Table 2. The governing conditions of the present study

slopes	Number of mesh	*Q(Lit/s)*	*V(m/s)*	*y(m)*
0	13100	3- 4.7- 6	0.159- 0.232-0.286	0.18-0.19-0.20
4:1	11500	3- 4.7- 6	0.159-0.232-0.286	0.18-0.19-0.20
8:1	12300	3- 4.7- 6	0.159-0.232-0.286	0.18-0.19-0.20
4:-1	10540	3- 4.7- 6	0.159-0.232-0.286	0.18-0.19-0.20
8:-1	11820	3- 4.7- 6	0.159-0.232-0.286	0.18-0.19-0.20

Table 3. Boundary conditions are governing the broad-crest weir with different crest slopes

AB	AD	BC	CD
Wall	Pressure- Inlet	Pressure- Outlet	Symmetry

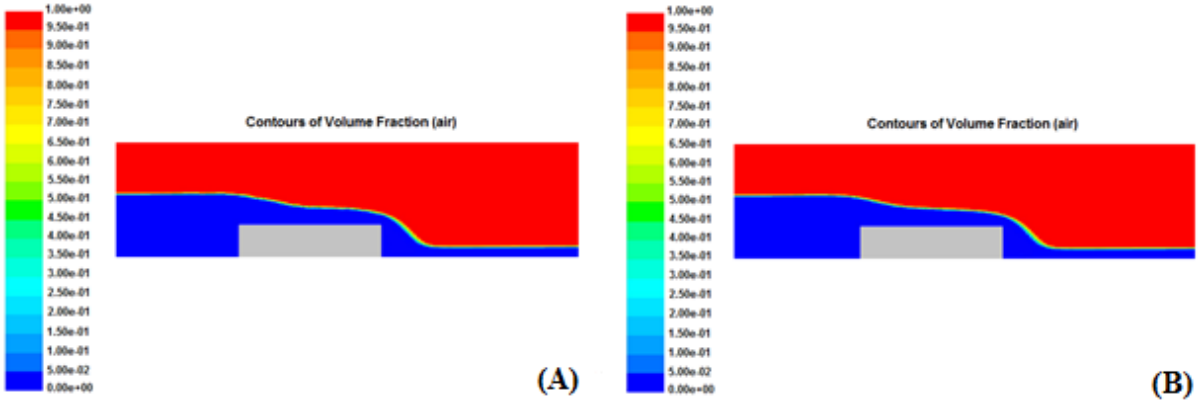

Fig. 4. The water-air contour of the flow over the broad-crest weir: A: Turbulence Model Standard k-ε, B: Turbulence Model RNG k-ε

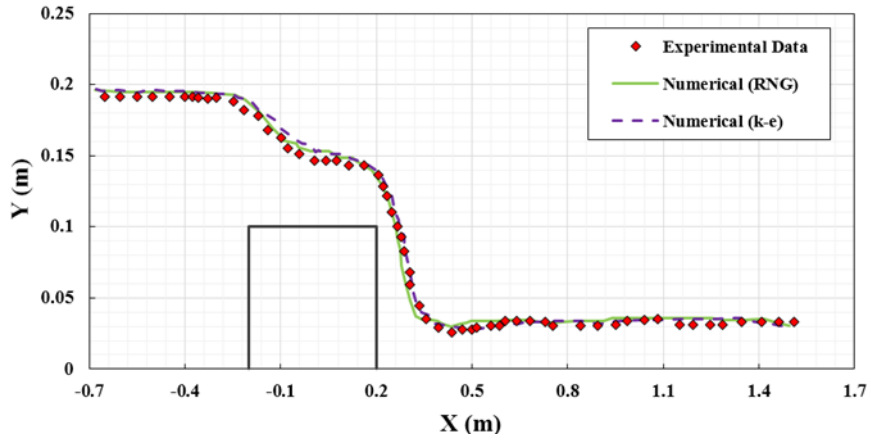

Fig. 5. Comparison of numerical and experimental results of water surface profile

broad-crest weir with 4.7 lit/s flow rate, respectively. The standard k-ε and RNG k-ε turbulence models is considered for simulation. In Fig. 5, the horizontal axis represents the longitudinal dimension of the channel and, the vertical axis represents the flow depth.

Table 4 shows two statistical indicators, Root Mean Squared Errors (RMSE) and Relative error (RE), which are used to compare numerical and experimental results of the water surface profile.

By comparing numerical and experimental data using the evaluation criteria of Table 4, it is observed that the RNG k-ε model in the simulation of the surface flow profile of a broad crested rectangular weir has the better operation than the standard k-ε turbulence model (Fig. 5). The relative error and RMSE error for the RNG k-ε turbulence model were %2.55, 0.27 cm and for the standard k-ε turbulence model

Table 4. Relationship of evaluation criteria

Evaluation criteria	Relationship
Root Mean Squared Errors	$RMSE = \sqrt{\frac{1}{n}\sum_{1}^{n}\left(X_{Exp} - X_{Cal}\right)^2}$
Relative Error	$RE = \frac{\left\|X_{Exp} - X_{Cal}\right\|}{X_{Exp}}$

Table 5. The value of the errors obtained from the turbulence models in the current research

Model	RE (%)	RMSE(cm)
RNG k-ε	2.55	0.27
Standard k-ε	5.03	0.57

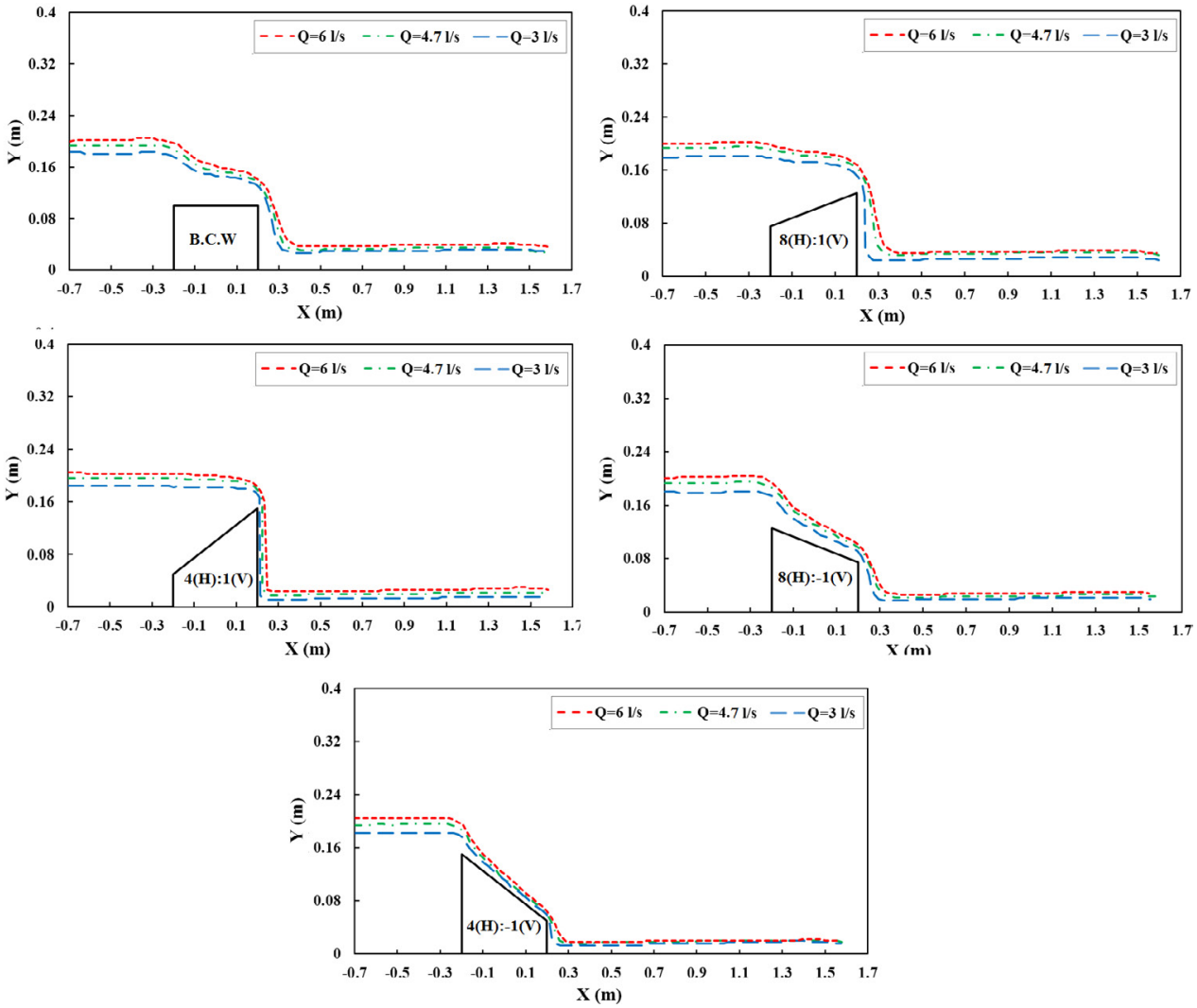

Fig. 6. Water surface profiles with different slopes of the broad-crest weir

were %5.03 and 0.57 cm, respectively. Results are presented in Table 5. The accurate performance of the RNG k-ε turbulence model in the simulation of flow through the weir and undergates is confirmed by previous researchers [28, 29, 30].

3-2- Water surface profiles with different sloped broad-crested weir

Fig. 6 shows the water surface profile of 3 discharges; 3, 4.7,6 lit/s for 5 different slopes (0:1, 4:1, 8:1, 4:-1, 8:-1) in the broad-crested weir.

According to Fig. 6, increasing the discharge, increases the flow depth. It should be noted that the flow depth at downstream of the weir is changed due to adverse or positive slope of the crest. In such a way that the downstream flow depth decreases by applying an adverse slope to the weir. This is due to the increase in the flow rate during overflowing the adverse sloped weir.

3-3- Changes the Froude number during the resolution range

In order to investigate the effect of different slopes of the broad-crested weir on the Froude number ($Fr = V/\sqrt{gy}$), Fig. 7 shows the changes in Froude number to the longitudinal dimension for the height of the weir body with different sizes.

It can be seen from Fig. 7 that the Froude number upstream of the broad-crested weirs are less than one; in other words, the flow is subcritical. In broad-crested weirs with positive slopped crest, the critical conditions (Fr = 1) has occurred on the weir crest toward the downstream. However, in weirs with an adverse slopped crest, the control section due to the separation of the flow at the apex and having entrapped air, occur slightly off the crest. Therefore, it is not recommended for discharge measuring weir to make adverse sloped crest. Table 6 shows the location of the control section on the broad-crest weir for different flow discharges. The location of the control section is normalized by Eq. (17).

$$X_{norm} = \frac{X - X_{\min}}{X_{\max} - X_{\min}} \tag{17}$$

In this relation, X_{norm} is the normalized longitudinal length of the weir crest X_{max} and X_{min} are the longitudinal dimension from the beginning to the upstream face and the downstream face of the weir crest, respectively.

According to Table 6, in zero or positive sloped crest, the control section occurs on the crest and for the adverse slope, the control section due to the separation of the flow at the beginning of the crest occurs outside of the crest. Also, by increasing the slope at the same discharge, the control section

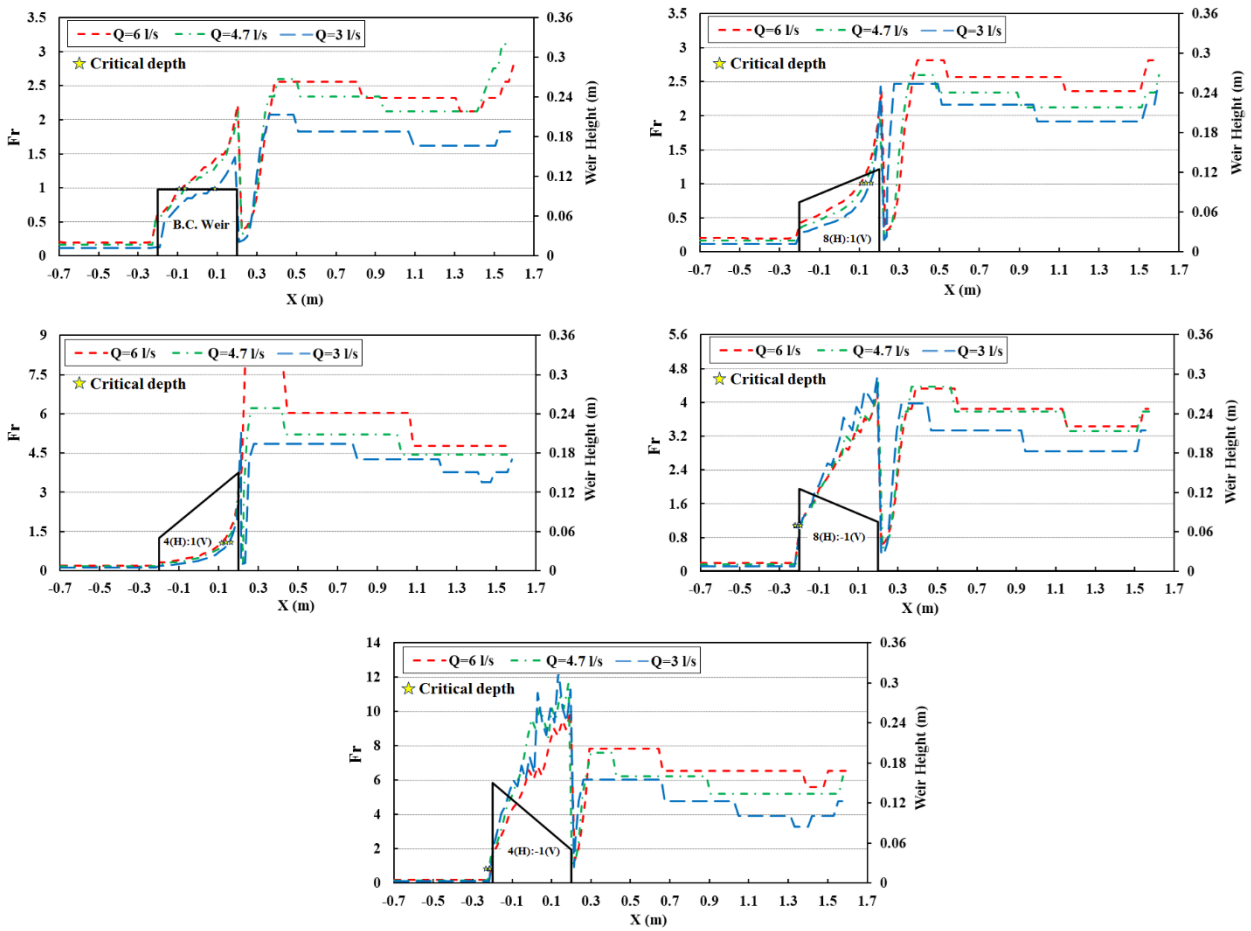

Fig. 7. The changes in Froude number to the longitudinal dimension for the height of the weir body with different sizes

Table 6. Normalized location of the control section on the broad-crested weir with different slopes

Slopes	Q(Lit/s)		
	3	4.7	6
0	0.742	0.337	0.307
4:1	0.865	0.803	0.762
8:1	0.874	0.815	0.764
4:-1	Out of crest range	Out of crest range	Out of crest range
8:-1	Out of crest range	Out of crest range	Out of crest range

Table 7. Average Froude number in downstream of the broad-crest weir

Slopes	Q(Lit/s)		
	3	4.7	6
0	1.64	2.15	2.21
4:1	4.22	4.90	5.82
8:1	2.04	2.08	2.32
4:-1	4.72	5.63	6.58
8:-1	3.02	3.53	3.56

moves towards the weir's downstream. In the Table 7, the average Froude number at downstream of the broad-crest weir is presented in terms of the weir's crest slope and the flow discharge. According to this table, due to decreasing the flow depth, positive and adverse slopes cause the increase in the Froude number at the downstream of the weir.

3-4- Total Energy Changes

For a section of flow, the total energy of the water is presented as Eq. (18).

$$H = z + \frac{P}{\gamma} + \frac{v^2}{2g} \tag{18}$$

In this relation, H presents the total energy, z presents the elevation load, P/γ presents the pressure load, and $v^2/2g$ presents the velocity load. P, g present the pressure and Special Weight parameters, respectively. Fig. 8 shows the total energy variation relative to the longitudinal dimension for different heights of the weir body.

It can be seen from Fig. 8 that, without considering the slope of the crest in a broad-crested weir, the total energy on the weir crest increases for all modes. In Table 8, the mean values of total energy in the downstream of the weir are presented. It can also be concluded that the total energy amount in the downstream of the weir is not a function of crest slope and increases the height of the weir and flow discharge from 3 to 6 liters per second. The maximum of total energy in the downstream of the weir for discharges of 3, 4.7 and 6 lit/s, occurs for slopes of 4:1, 4:-1 and 8:-1 which are 0.244, 0.317 and 0.452, respectively.

4. CONCLUSION

In this research, numerical analysis of the effect of the broad sloped crest on the hydraulic characteristics of the flow such as water surface profile, Froude number, the critical depth location (control section) and total energy using the Fluent software was investigated. Gambit software was used to make a range of solutions and generate the mesh. To simulate the free flow surface, the volume of fluid (VOF) method was used and for the turbulence, standard K-ε and RNG k-ε models along with different weir crest slopes and three flowrates were used. The results are as follows:

1. The RNG k-ε turbulence model in the simulation of the rectangular broad crest weir's surface-flow profile act better than the standard k-ε model.
2. By applying a adverse or positive slope to the weir crest, the flow depth at the downstream of the weir changes. Decreasing the flow depth with the increase of the crest slope, especially the adverse slope, is tangible. This is due to the increase of the flow rate during overflow from the adverse slope weir.
3. In the broad-crest weirs with zero or positive slope the control section occurs on the crest and for the adverse

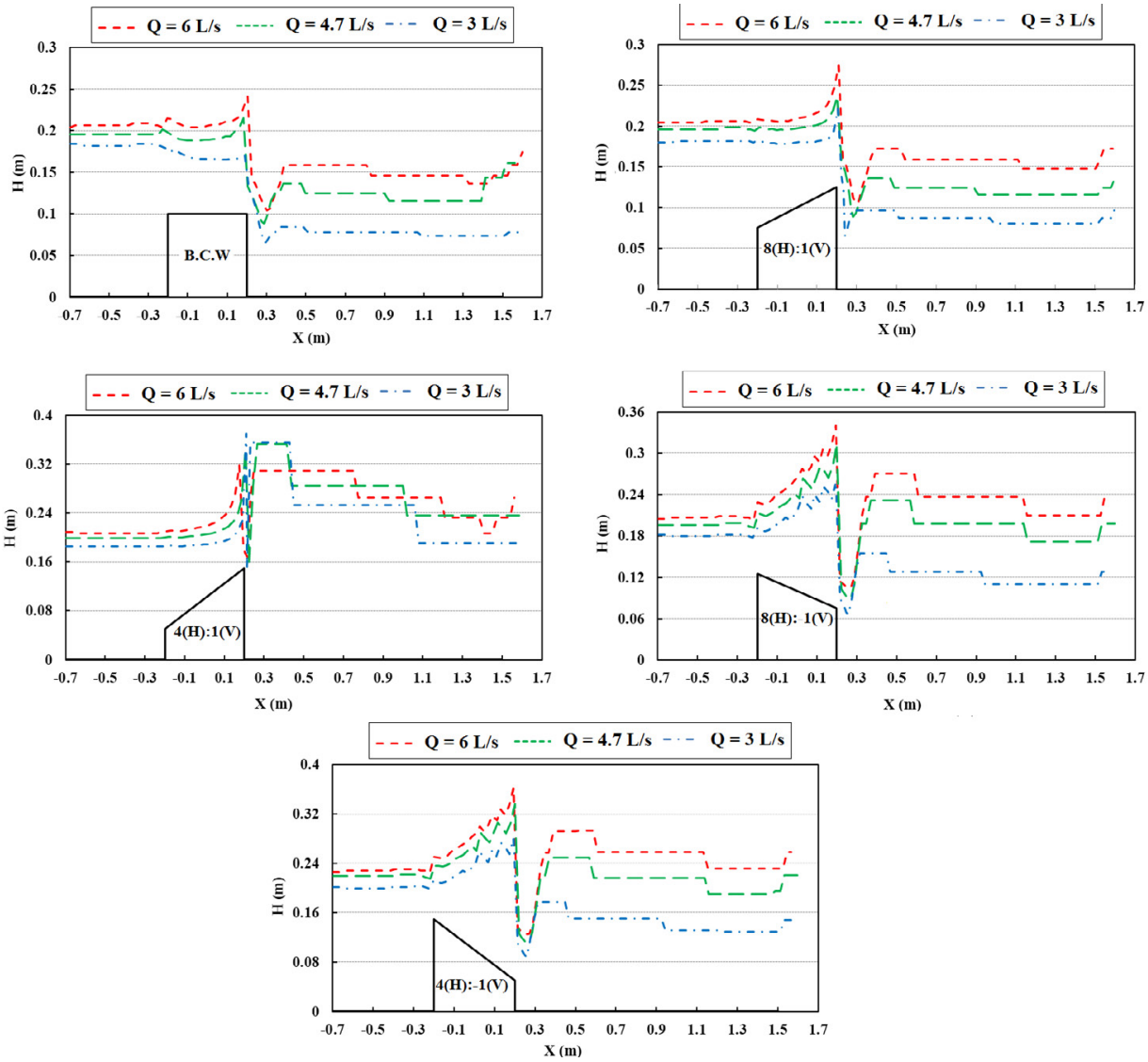

Fig. 8. The total energy changes over the longitudinal dimension for different weir's heights

Table 8. The mean total energy in downstream of the broad-crest weir

Slopes	Q(Lit/s)		
	3	4.7	6
0	0.079	0.123	0.147
4:1	0.244	0.269	0.270
8:1	0.087	0.121	0.154
4:-1	0.191	0.317	0.453
8:-1	0.120	0.188	0.223

slope, the control section due to the separation of the flow at the beginning of the crest occurs outside the crest.

4. By increasing the slope in a constant discharge, the control section moves towards the downstream of the weir. Also, with increasing the discharge for a constant (adverse and positive) slope, the mean Froude number in downstream,

of the weir increases.

5. Total energy along the weir's crest from the upstream to the downstream of the crest increases, regardless of the slope.
6. The total energy in downstream of the weir is not a function of the crest slopes. The total energy increases with increasing the height of the weir's body and flow discharges from 3 to 6 lit/s. The highest amount of the total energy in downstream of the weir occurs for discharges of 3, 4.7 and 6 lit/s with the slopes of 4:1, 4:-1, 8:-1 and are 0.244, 0.317 and 0.452, respectively.
7. The steepening of the weir's slopes lead to an increase in the total energy in downstream of the weir.
8. The results of this study show that with weir crest sloped adverse and positive, weir performance is better for positive and flow control over weir, which is applicable to construction projects.

5. Nomenclature

Q	Weir flow discharge, l/s
H_0	Energy head, m
h_0	Water depth at upstream of the weir, m
y_0	The approach weir depth, m
y_c	The Critical depth, m
S	Height of weir, m
L_w	Length of weir crest, m
P	Total pressure, N/m^2
Fr	Froude number
g	Gravitational acceleration, m/s^2
V	Velocity, m/s
θ	Ratio of the vertical slope to the horizontal slope
ρ	Density, kg/m^3
μ	Dynamic viscosity, kg/m.s
γ	Special Weight, N/m^3
S_{ij}	The stress tensor, N/m^2
v_t	The eddy viscosity, m^2/s
ε	Turbulent dissipation, m^2/s^3
k	Turbulent kinetic energy, m^2/s^2
i	Unit in x direction
j	Unit in y direction
x	Direction

REFERENCES

[1] H. A Doeringsfeld, C. L. Baker, Pressure-momentum theory applied to the broad-crested weir, Trans, ASCE, 106 (1941) 934-969.

[2] H. J. Tracy, Discharge characteristics of broad-crested weirs, U.S. Geol. Survey, Circular, 397 (1957) 1-15.

[3] F. M. Henderson, Open channel flow, Macmillan, New York, 1966.

[4] S. S. Rao, M. K. Shukla, Characteristics of flow over weirs of finite crest width, Journal of the Hydraulics Division, 97(11) (1971) 1807-1816.

[5] M. G. Bos, A. J. Clemmens, J. A. Replogle, Flow measuring flumes for open channel systems, Wiley, New York, 1984.

[6] A. S. Ramamurthy, U. S. Tim, M. V. J. Rao, Characteristics of square-edged and round-nosed broad-crested weirs, Journal of Irrigation and Drainage Engineering, 114(1) (1988) 61-73.

[7] W.H. Hager, M. Schwalt, Broad-crested weir, J. Irrig. Drain. Engine, 120(1) (1994) 13-26.

[8] H.M. Fritz, W. H. Hager, Hydraulics of embankment weirs, J. Hydraul. Eng, 124(9) (1998) 963–971.

[9] M.C. Johnson, Discharge coefficient analysis for flat-topped and sharp-crested weirs, Irrigation science, 19(3) (2000) 133-137.

[10] J. Farhoudi, H. Shahalami, Slope effect on discharge efficiency in rectangular broad crested weir with sloped upstream face, Int. J. Civ. Eng., 3(1) (2005) 58-65.

[11] M. Gogus, Z. Defne, V. Ozkandemir, Broad-crested weirs with rectangular compound cross sections, J. Irrig. Drain. Eng, 132(3) (2006) 272–280.

[12] D.M. Hargreaves, H.P. Morvan, N.G. Wright, Validation of the volume of fluid method for free surface calculation: the broad crested weir, Engineering Applications of Computational Fluid Mechanics, 1(2) (2007) 136–146.

[13] J. Farhoudi, N. Shokri, Flow from broad crested rectangular weirs with sloped downstream face, 32nd IAHR Congress, Venice, Italy, 2007.

[14] J. E. Sargison, A. Percy, Hydraulics of broad-crested weirs with varying side slopes, Journal of irrigation and drainage engineering, 135(1) (2009) 115-118.

[15] E. Goodarzi, J. Farhoudi, N. Shokri, Flow characteristics of rectangular broad-crested weirs with sloped upstream face, Journal of Hydrology and Hydromechanics, 60(2) (2012) 87-100.

[16] S. H. Hoseini, Experimental investigation of flow over a triangular broad-crested weir, ISH Journal of Hydraulic Engineering, 20(2) (2014) 230-237.

[17] M. A .Torabi, M. Shafieefar, An experimental investigation on the stability of foundation of composite vertical breakwaters, Journal of Marine Science and Application, 14(2) (2015) 175-182.

[18] N. O. Tănase, D. Broboană, C. Bălan, Free surface flow over the broad-crested weir, In 2015 9th International Symposium on Advanced Topics in Electrical Engineering (ATEE), IEEE, (2015) 548-551.

[19] J. Mohammadzadeh-Habili, M. Heidarpour, A. Haghiabi, Comparison the hydraulic characteristics of finite crest length weir with quarter-circular crested weir, Flow Measurement and Instrumentation, 52 (2016) 77-82.

[20] T. Xu, Y. C. Jin, Numerical Study of the Flow over Broad-Crested Weirs by a Mesh-Free Method, Journal of Irrigation and Drainage Engineering, 143(9) (2017) 04017034.

[21] A. Parsaie, H. M.Azamathulla, A. H. Haghiabi, Prediction of discharge coefficient of cylindrical weir–gate using GMDH-PSO, ISH Journal of Hydraulic Engineering, 24(2) (2018) 116-123.

[22] R. Daneshfaraz, O. Minaei, J. Abraham, S. Dadashi, A. Ghaderi, 3-D Numerical simulation of water flow over a broad-crested weir with openings, ISH Journal of Hydraulic Engineering, (2019) 1-9.

[23] R. Daneshfaraz, B. Kaya, Solution of the propagation of the waves in open channels by the transfer matrix method. Ocean Engineering, 35(11-12) (2008) 1075-1079.

[24] P. Suhas, Numerical Heat Transfer and Fluid Flow". Hemisphere Publishing Corporation, Taylor and Francis Group, New York, (2012) 11-23.

[25] V. Yakhot, S. A. Orszag, S. Thangam, T. B. Gatski, C. G. Speziale, Development of turbulence models for shear flows by a double expansion technique, Physics of Fluids A: Fluid Dynamics, 4(7) (1992) 1510-1520.

[26] H. Zahabi, M. Torabi, E. Alamatian, M. Bahiraei, M. Goodarzi, Effects of Geometry and Hydraulic Characteristics of Shallow Reservoirs on Sediment Entrapment, Water, 10(12) (2018) 1725.

[27] M. A. Sarker, D. G. Rhodes, Calculation of free-surface profile over a

rectangular broad-crested weir, Flow measurement and Instrumentation, 15(4) (2004) 215-219.

[28] R. Daneshfaraz, A. Ghahramanzadeh, A.Ghaderi, A. R. Joudi, J. Abraham, Investigation of the Effect of Edge Shape on Characteristics of Flow under Vertical Gates, Journal-American Water Works Association, 108(8) (2016) 425-432.

[29] R. Daneshfaraz, A. Ghaderi, Numerical Investigation of Inverse Curvature Ogee Weir, Civil Engineering Journal, 3(11) (2017) 1146-1156.

[30] R. Daneshfaraz, A.R. Joudi, A. Ghahramanzadeh, A. Ghaderi, Investigation of flow pressure distribution over a stepped spillway. Advances and Applications in Fluid Mechanics, 19(4) (2016) 811.

HOW TO CITE THIS ARTICLE

R. Daneshfaraz, M. Dasineh, A. Ghaderi, S. Sadeghfam, Numerical Modeling of Hydraulic Properties of Sloped Broad Crested Weir, AUT J. Civil Eng., 4(2) (2020) 229-240.

DOI: 10.22060/ajce.2019.16184.5574